

No need for a grid: Adaptive fully-flexible gaussians for solving the time-dependent Schrödinger equation

Simen Kvaal,^{1,2,*} Caroline Lasser,^{1,3} Thomas Bondo Pedersen,^{1,2} and Ludwik Adamowicz^{1,4}

¹*Centre for Advanced Study at the Norwegian Academy of Science and Letters, Drammensveien 78, N-0271 Oslo, Norway*

²*Hylleraas Centre for Quantum Molecular Sciences,
Department of Chemistry, University of Oslo, Norway*

³*Zentrum Mathematik, Technische Universität München, München, Germany*

⁴*Department of Chemistry and Biochemistry, University of Arizona, Tucson, Arizona 85721, USA*

(Dated: 7 March 2023)

Linear combinations of complex gaussian functions, where the linear and nonlinear parameters are allowed to vary, are shown to provide an extremely flexible and effective approach for solving the time-dependent Schrödinger equation in one spatial dimension. The use of flexible basis sets has been proven notoriously hard within the systematics of the Dirac–Frenkel variational principle. In this work we present an alternative time-propagation scheme that de-emphasizes optimal parameter evolution but directly targets residual minimization via the method of Rothe’s method, also called the method of vertical time layers. We test the scheme using a simple model system mimicking an atom subjected to an extreme laser pulse. Such a pulse produces complicated ionization dynamics of the system. The scheme is shown to perform very well on this model and notably does not rely on a computational grid. Only a handful of gaussian functions are needed to achieve an accuracy on par with a high-resolution, grid-based solver. This paves the way for accurate and affordable solution of the time-dependent Schrödinger equation for atoms and molecules within and beyond the Born–Oppenheimer approximation.

I. INTRODUCTION

When atoms and molecules are subjected to ultrashort and intense laser pulses, their wave functions become highly complicated and fast-changing due to ionization and fragmentation processes [1]. High spatial and temporal resolutions and large computational domains are mandatory when the time-dependent Schrödinger equation (TDSE) is solved numerically, and computational approaches that, at some level, are based on the Born–Oppenheimer approximation may no longer be appropriate. For even the most modestly sized atoms, it is simply impossible to achieve experiment-level accuracy with a grid or an otherwise fixed basis due to the curse of dimensionality of the problem. Therefore, it is essential to develop compact and flexible wave-function representations that can be efficiently propagated in a numerically stable manner.

This work has two main aims: The first is to demonstrate that gaussian functions with time-evolving complex parameters form a very flexible and efficient basis set to represent complicated wave-function dynamics. The second is to present a computational method for optimizing the nonlinear parameters of the gaussians whilst changing their number as needed during the simulation. As an initial test, we consider a 1D model problem mimicking a hydrogenic atom or ion subjected to an ultrashort laser pulse that induces rather extreme dynamics, including ionization. With the new time-propagation scheme based on nonlinear least-squares optimization, we

show that a compact gaussian basis set can reproduce the essentially exact grid-based reference solution of the TDSE for our model problem. In particular, the ionization tail of the wave function is very well captured at every stage of the dynamics using only a handful of the complex gaussians.

Using a linear combination of gaussians (LCG) *Ansatz* with complex and in particular explicitly correlated parameters is well established for highly accurate calculations of bound states of small atoms and molecules using the Rayleigh–Ritz variational method [2]. Notably, some of these applications have been performed *without* assuming the Born–Oppenheimer approximation, i.e., treating the motion of the nuclei and electrons on an equal footing. An attractive feature of the LCG *Ansatz* is the existence of analytic formulas for matrix elements involving complex gaussians, including the explicitly correlated ones [3].

The time-dependent Dirac–Frenkel principle [4–7] appears as a natural framework for a dynamical extension of the variational LCG approach to bound states. The Dirac–Frenkel principle, however, has a notorious problem with severely ill-conditioned or even singular Gramian matrices [8]. This problem is particularly acute for LCG wave functions [9] and yields to the frozen width of the gaussians and an additional Thykonov regularization in the variational multi-configurational gaussian (vMCG) [10] method. Regrettably, the great flexibility of the complex gaussians comes at a prize.

The alternative time-propagation scheme proposed in this work averts the matrix singularity problem of the Dirac–Frenkel principle by using Rothe’s method, also called the method of vertical time layers [11, 12], for solving the TDSE. The Rothe method is a variational

* simen.kvaal@kjemi.uio.no

approach that, in a natural manner, allows for adaptivity of the size of the gaussian basis set during the time-propagation of the wave function: The number of gaussians is increased whenever the error in the wave function becomes too large. Moreover, the method is entirely formulated in terms of the gaussian matrix elements of certain operators and their derivatives with respect to the nonlinear parameters of the gaussians. Thus, the method *completely eliminates* the need for a grid, while allowing the wave function to freely roam space with, in principle, infinite level of detail.

The compression levels observed with LCG wave functions for the 1D case in the present work may be even more pronounced for multi-particle systems with the use of N -particle explicitly correlated gaussians that have been routinely employed in calculating bound spectra of small atoms and molecules with very high accuracy. The method presented here thus paves the way for highly accurate solutions of the TDSE for realistic chemical systems, including ionization and dissociation processes induced by sub-femtosecond laser pulses, employing neither a grid nor a fixed basis expansion of the wave function.

II. THEORY

A. Complex gaussians

We first consider the general case of a quantum system composed of N charged particles (e.g., a non-Born–Oppenheimer description of a molecule with nuclei and electrons moving in a central potential [13]) whose Cartesian coordinates are collected in a $3N$ -dimensional real vector \mathbf{r} . An LCG(K) wave-function *Ansatz* (prior to spin and permutation-symmetry adaptation) at time t is expressed in terms of K N -particle complex gaussians in the following way:

$$\psi(\mathbf{r}, t) = \sum_{k=1}^K c_k(t) \exp[-(\mathbf{r} - \mathbf{s}_k(t))' \mathbf{C}_k(t) (\mathbf{r} - \mathbf{s}_k(t))]. \quad (1)$$

Here, c_k is a complex linear coefficient, \mathbf{s}_k is a complex shift vector, and \mathbf{C}_k is a $3N \times 3N$ matrix of complex parameters. Note that all parameters, nonlinear as well as linear, are time-dependent. Here and in the following, the prime denotes vector and matrix transposition (without complex conjugation). Both the real and imaginary parts of $\mathbf{C}_k = \mathbf{a}_k + i\mathbf{b}_k$ are real symmetric $3N \times 3N$ matrices. The real part must be constrained to be symmetric positive definite to ensure square-integrability. An alternative (but equivalent) functional form of the gaussians in Eq. (1) is

$$g_k(\mathbf{r}) = \exp\left[-\frac{1}{2}(\mathbf{r} - \mathbf{q}_k)' \mathbf{C}_k (\mathbf{r} - \mathbf{q}_k) + i\mathbf{p}_k' (\mathbf{r} - \mathbf{q}_k)\right], \quad (2)$$

with real vectors \mathbf{q}_k and \mathbf{p}_k defining the center and momentum of the gaussians, respectively.

Both the linear expansion coefficients *and* the nonlinear parameters of each gaussian are free variables that can be optimized in the calculation. In Eqs. (1) and (2) the exponent is a general second-order polynomial with respect to the complex parameters, up to an irrelevant constant. As is well known, the family of gaussian functions is complete in more than one sense [14, 15]. Therefore, choosing even a modest K value with freely adjustable nonlinear parameters should form an inordinately flexible basis set to represent almost any wave function.

Importantly, integrals for the matrix elements of the kinetic and potential energies and the overlap have explicit analytic formulas that can be straightforwardly implemented in an efficient computer code. For example, unshifted complex gaussians satisfy

$$\langle g_k | r_{ij}^{-1} | g_l \rangle = \frac{2 \langle g_k | g_l \rangle}{\sqrt{\pi \operatorname{tr}((\mathbf{C}_k + \mathbf{C}_l)^{-1} \mathbf{J}_{ij})}},$$

where $r_{ij} = |\mathbf{r}_i - \mathbf{r}_j|$ and \mathbf{J}_{ij} is the matrix associated with the quadratic form $r_{ij}^2 = \mathbf{r}' \mathbf{J}_{ij} \mathbf{r}$ [3, 16]. Such analytic formulas pave the way for developing a completely grid-free gaussian time-propagation approach.

B. The Rothe method

The time-dependent Schrödinger equation can be phrased in a variational form as

$$\dot{\psi}(t) = \underset{\chi}{\operatorname{argmin}} \|i\chi - \hat{H}(t)\psi(t)\|, \quad (3)$$

where χ ranges over all allowed infinitesimal variations of $\psi(t)$. For some approximate *Ansatz* depending smoothly on a set of (real) parameters, the variations are restricted, leading to an implicit system of ODEs for the parameters. This is the first step of the Dirac–Frenkel variational principle. In the next step, the ODEs are integrated using some numerical integration scheme. It should be noted, however, that time-propagation with the Dirac–Frenkel principle is infamous for its numerical challenges [8], which are particularly pronounced for LCG *Ansätze*, see for example [9, 17]. While successful work-arounds have emerged, including the frozen gaussian approximation [10] and sophisticated basis re-expansion techniques [18–23], no general approach that can fully exploit the high flexibility of complex gaussians to simulate complicated quantum dynamics has been formulated.

Somewhat paradoxically, it is the high flexibility of the complex gaussians that causes the numerical challenges. There may be several distinct LCGs that approximate the same wave function to a similar accuracy—i.e., there is no unique set of the gaussians and, thus, no unique set of their nonlinear parameters. This leads to the system of ODEs being insoluble due to singular or severely ill-conditioned Gramian matrices, which present a challenge that is significantly harder to overcome than ordinary “stiffness”.

Rothe's method offers a different approach than the Dirac–Frenkel principle. Placing all focus on the *total time-evolving wave function*, Rothe's method de-emphasizes the evolution of the nonlinear gaussian parameters and the linear expansion coefficients. Equation (3) is discretized *first* in the time variable by some suitable scheme. For example, using the *implicit trapezoidal rule* and time step h , the wave function at time $t_n = nh$ is:

$$\psi^n = \underset{\varphi}{\operatorname{argmin}} \|\mathcal{A}_n \varphi - \mathcal{A}_{n-1}^\dagger \psi^{n-1}\|, \quad (4)$$

where $\mathcal{A}_n = I + ih\hat{H}(t_n)/2$ and $\psi^n \approx \psi(t_n)$ is an approximation to the wave function at time t_n . This turns the propagation into a sequence of nonlinear optimization problems. Although any other scheme can be chosen instead, the trapezoidal rule is a rather natural starting point, see also [24]. In particular, the exact solution to the time-propagation equation (4) in the Hilbert space is given by the Crank–Nicolson (CN) scheme [25], whose local error is $O(h^3)$.

Using the time-discretized version of the time-dependent variational principle in Eq. (4), one can now introduce an *Ansatz*, e.g., the LCG(K) wave function, at each time t_n , $\psi^n = \psi(\alpha^n, c^n)$. Here, α^n and c^n denote the sets of nonlinear and linear parameters, respectively, at time t_n . Some restrictions need to be imposed on the wave-function optimization problem to control the error in the calculation. A tolerance $\epsilon > 0$ is chosen and used in the propagation of the LCG wave function, $\psi(\alpha^n, c^n)$:

$$\frac{1}{2} \|\mathcal{A}_n \psi(\alpha^n, c^n) - \mathcal{A}_{n-1}^\dagger \psi(\alpha^{n-1}, c^{n-1})\|^2 < \epsilon. \quad (5)$$

The completeness of the gaussians ensures that the tolerance ϵ can always be achieved with an adaptive number of gaussians in the basis set. Hence, our propagation scheme for the LCG ansatz from time t_{n-1} to t_n needs to include a procedure for augmenting the gaussian basis set with additional functions.

The problem (5) is separable in the sense that freezing α^n results in a *linear* least-squares problem for c^n , see [26]. This leads to a reduced problem defined only in terms of finding a set of nonlinear parameters α^n such that

$$F(\alpha^n) = \frac{1}{2} \|(I - P_{\mathcal{A}_n}) \mathcal{A}_{n-1}^\dagger \psi(\alpha^{n-1}, c^{n-1})\|^2 < \epsilon. \quad (6)$$

Here, $P_{\mathcal{A}_n} = P_{\mathcal{A}_n}(\alpha^n)$ is an orthogonal projector on the space spanned by the gaussians transformed with the \mathcal{A}_n operator, and thus an explicit function of the unknowns α^n . Elimination of c^n is essential, as dependent variables in a nonlinear least-squares problem often lead to ill-conditioning of the problem [26].

Our nonlinear optimization scheme is a variant of the iterative Gauss–Newton method with step-size control via a simple Armijo backtracking strategy to ensure sufficient decrease of the objective function in each iteration [27, 28]. The Gauss–Newton method requires solution of a linear system in each iteration, and approaches

quadratic convergence when the objective function becomes small. A successful use of the Newton method for solving the equation $\nabla F(\alpha^n) = 0$ relies on providing a sufficiently good initial guess at the start of the calculation. In our approach, we reuse the optimized nonlinear parameters α^{n-1} obtained for t_{n-1} as the initial guess for the parameters at t_n . This usually works quite well and improves when the time step is lowered. However, the nonlinear optimization routine may get trapped in a local minimum with $F(\alpha^n) \geq \epsilon$. In such a case, we add one or more gaussians to the basis set. Our chosen strategy for the basis-set enlargement is fairly simple, but works quite well in the test simulation reported below. The nonlinear parameters of a gaussian are completely determined by the expectation values of position, momentum, position variance, and momentum variance. The residual expression, $f(\mathbf{r})$ (i.e., the function that appears inside the norm bars of $F(\alpha^n)$), provides the function for which the above-mentioned expectation values are calculated. Next, a gaussian is generated whose expectation values match the expectation values determined for $f(\mathbf{r})$. That gaussian is added to the LCG basis set and a complete optimization is performed for all gaussians in the enlarged basis set. If still $F(\alpha^n) \geq \epsilon$, a second gaussian is added to the basis set using the same procedure as used for adding the first gaussian. This addition process continues until $F(\alpha^n) \leq \epsilon$. The calculation then proceeds to the next time step.

III. NUMERICAL RESULTS

We use a simple one-dimensional (1D) model system to perform a proof-of-principle test simulation, which is simple enough to allow detailed analysis of the results while challenging enough to be impossible to carry out with conventional, straightforward techniques based on the Dirac–Frenkel variational principle.

A. 1D model system

We consider the simplest possible model system for a proof-of-principle study of the Rothe method applied to an LCG *Ansatz*: a one-dimensional, one-particle system. The Hamiltonian is defined by

$$\hat{H}(t) = -\frac{1}{2} \frac{\partial^2}{\partial x^2} + V(x) + x\mathcal{E}(t), \quad (7)$$

where $V(x) = -(1/2)/\sqrt{x^2 + 1/4}$ mimics the nuclear potential for the electron in a hydrogen atom. The ground-state energy in this potential is conveniently located at $E_0 = -1/2$. Note that atomic units are used throughout except where explicitly indicated otherwise. The time-dependent electric field $\mathcal{E}(t)$ is nonzero only in the

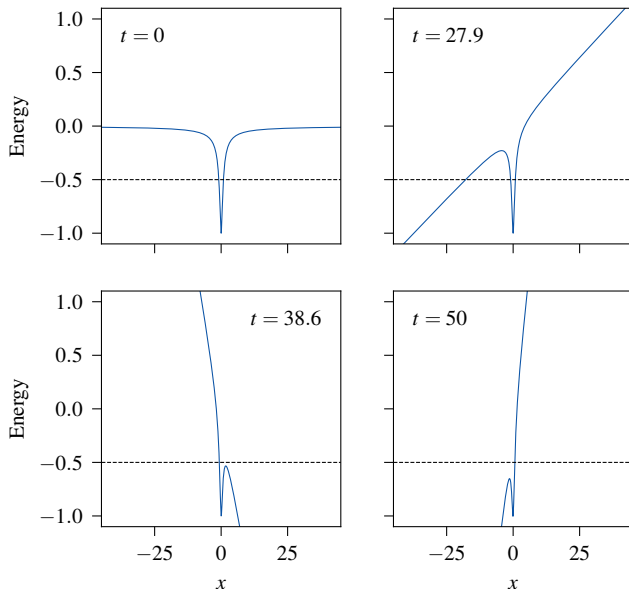


FIG. 1. The effective potential $V(x) + x\mathcal{E}(t)$ at the extrema of the electric field during the first half of the pulse. The horizontal dashed line indicates the ground-state energy of the potential $V(x)$.

$t_0 < t < t_1$ region, where it becomes equal to:

$$\mathcal{E}(t) = \mathcal{E}_0 \sin^2 \left(\pi \frac{t - t_0}{t_1 - t_0} \right) \cos(\omega(t - \bar{t})), \quad \bar{t} = \frac{t_0 + t_1}{2}. \quad (8)$$

In our model, we set $\omega = 0.25$ (6.8 eV, 182 nm), $t_0 = 20$, and $t_1 = 80$ (foot-to-foot duration 1.45 fs). The maximum amplitude of the field is $\mathcal{E}_0 = 0.225$ (116 V/nm) and occurs at $t = 50$, corresponding to peak intensity 18×10^{14} W/cm² and ponderomotive energy 0.203. The Keldysh parameter is $\gamma = 1.11$, which is traditionally interpreted as indicating predominance of multiphoton ionization over tunnel ionization. We stress that the laser-pulse parameters are chosen to generate complicated quantum dynamics, *not* to emulate a particular experimental setup. As is evident from the effective potential plotted at the extrema of the electric field in Fig. 1, the laser pulse violently disrupts the potential and certainly will induce significant ionization probabilities.

A highly accurate grid reference calculation is performed by spatially discretizing the real axis using a grid with $n_{\text{grid}} = 4096$ equidistant points in the interval $[-l, l] = [-500, 500]$. The kinetic-energy part is approximated using the standard Fast Fourier Transform (FFT) approach. This approach introduces artificial periodic boundary conditions, which have negligible effect on the results due to the large domain used in the calculations. The time evolution can be carried out in a number of ways. In the present work we choose the well-known Crank–Nicolson (CN) scheme [25] with the time step $h = 10^{-3}$, since our proposed LCG propaga-

tion scheme is an approximation to that scheme.

The initial wave function is the ground state of the model potential $V(x)$ obtained by inverse iterations with the conjugate gradient method [25]. It is shown in Fig. 2 along with the complete history of the propagation of the essentially exact grid-based wave function $\psi_{\text{CN}}(x, t)$ and the final wave function, $\psi_{\text{CN}}(x, 100)$. As one can see, the final wave function spreads over more than 200 bohrs with highly oscillatory real and imaginary parts associated with ionization. As can be seen in the propagation history in the middle panel of Fig. 2, the spreading of the wave function proceeds in accordance with the effective-potential oscillations depicted in Fig. 1. As expected on physical grounds, the wave function continues to spread after the laser is switched off at $t = 80$.

B. Rothe propagation of an LCG Ansatz

In order to compare the proposed LCG propagation scheme to the grid-based Crank–Nicolson simulation above, we need to use (very nearly) identical initial wave functions. Therefore, we compute the LCG ground-state wave function by a nonlinear least-squares fit to the grid-based initial state using an LCG(4) Ansatz, $\psi_{\text{gs},4}$, on the form (2) specialized to one spatial dimension. Figure 3 shows the resulting local error of $\psi_{\text{gs},4}$. The real parameters of the four gaussians are: $q_i = p_i = b_i = 0$ and $a = [0.37745, 2.0681, 0.61766, 1.0688]$, and the linear coefficients are: $c = [0.08719, 0.061077, 0.29305, 0.23122]$. The fitting error is $\|\psi_{\text{gs}} - \psi_{\text{gs},4}\|^2 = 4.3485 \times 10^{-7}$. The LCG(4) ground-state energy thus is accurate to around 7 digits.

We use the same time step as in the grid-based CN simulation, $h = 10^{-3}$, and select the threshold $\epsilon = 10^{-7}$ for the nonlinear least-squares optimization in the Rothe LCG simulation. The value of the threshold is chosen so that the global error in the scheme is comparable to that used in the grid-based CN simulation. In the present implementation the gaussian matrix elements are evaluated using quadrature that is sufficient (and nearly exact) for the 1D model considered in the present calculations.

The Gauss–Newton iterative method involves the numerical solution of linear systems of comparable size and structure as those required for evaluating the parameter time-derivatives in the Dirac–Frenkel principle. As the calculation progresses, the Gauss–Newton method uses a single iteration in the vast majority of the time steps (it uses two iterations in a tiny fraction of the time steps, and three and nine iterations in only two time steps). In contrast to the Dirac–Frenkel principle, the conditioning of the linear systems does not seem to be a problem. The time propagation produces near-smooth paths for all gaussians except where functions are added. At those points, the reoptimization of all the non-linear parameters of all gaussians requires varying numbers of iterations, but they always converge without a problem. In Fig. 4, the objective function $F(\alpha^n)$ is shown, together

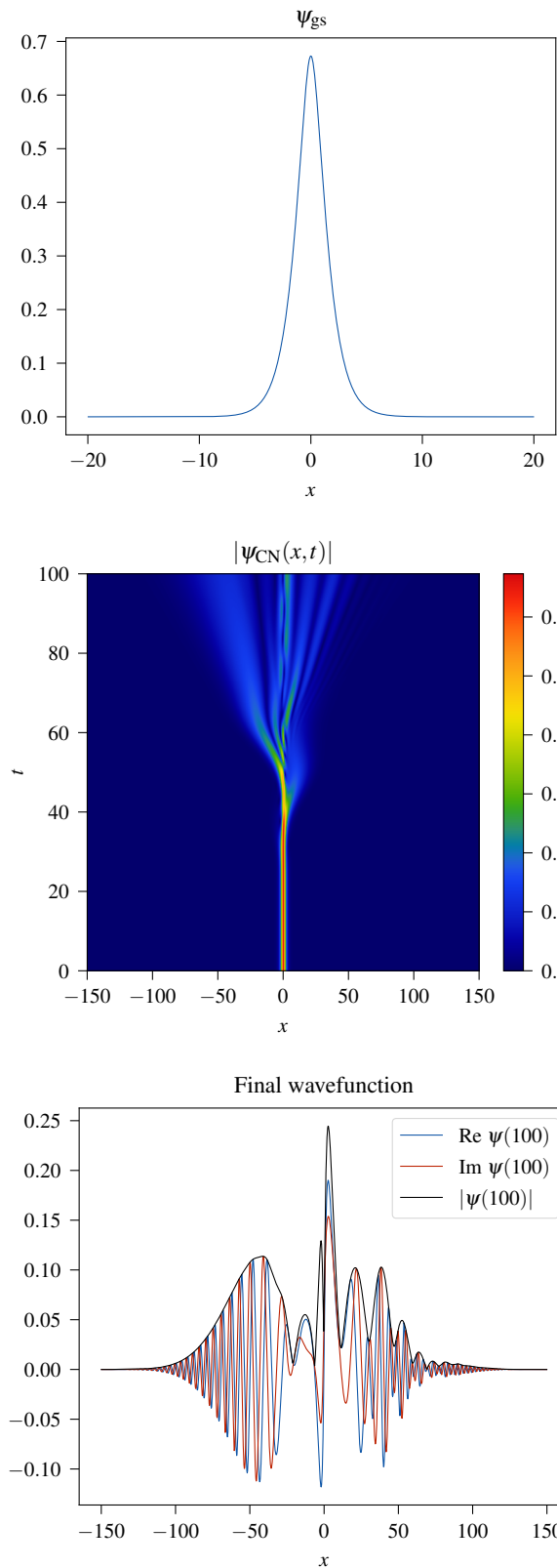


FIG. 2. The initial wave function (top), the propagation history of the model system (middle), and the final wave function (bottom). The propagation is performed on a fine spatial grid using the Crank–Nicolson method with time step $h = 10^{-3}$.

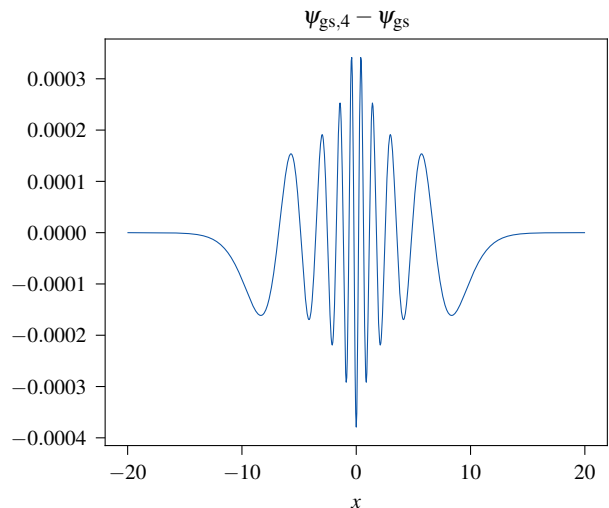


FIG. 3. The local error of $\psi_{gs,4}$, which is an LCG(4) least-squares fit to the grid-based ground-state wave function shown in Fig. 2.

with the number of gaussians needed to achieve the convergence criterion, $F(\alpha^n) < \epsilon$, as a function of time. The number of functions increases throughout the simulation with a modest value of $K = 18$ at the final time $t = 100$.

The local error of the LCG propagation relative to the grid-based CN propagation is shown in Fig. 5. The density plot corresponding to the middle panel of Fig. 2 is not shown, as the local errors are too small to make the plots visibly different. The log-scale plot of the local error, Fig. 6, reveals that errors are present, but, in general, they have very small values.

The final LCG and CN wave functions are compared in Fig. 6, which reveals that the largest errors occur around $x = 0$. Still, the largest errors are an order of magnitude lower than the errors in the ground-state wave function, Fig. 3.

For each time step, on average, the most time consuming part of the calculation is solving a set of linear equations with the dimension equal to the number of non-linear wave-function parameters. In the present simulations, the number of gaussians needed to meet the error tolerance ranges between $K = 4$ and $K = 18$. Hence, the linear systems to be solved are small, and a very accurate representation of the highly oscillatory and delocalizing dynamics of the 1D model system is obtained. We note in passing that for three-dimensional systems of (sets of) identical particles, where the correct spin and permutation symmetries must be treated explicitly, the computational bottleneck of each time step will likely be the evaluation of integrals over the gaussians rather than solving the least-squares problem (6).

The performance of the present method compares favorably with state-of-the-art methods for the ab initio simulation of small atoms and molecules in terms of efficiency and error control. For example, methods employ-

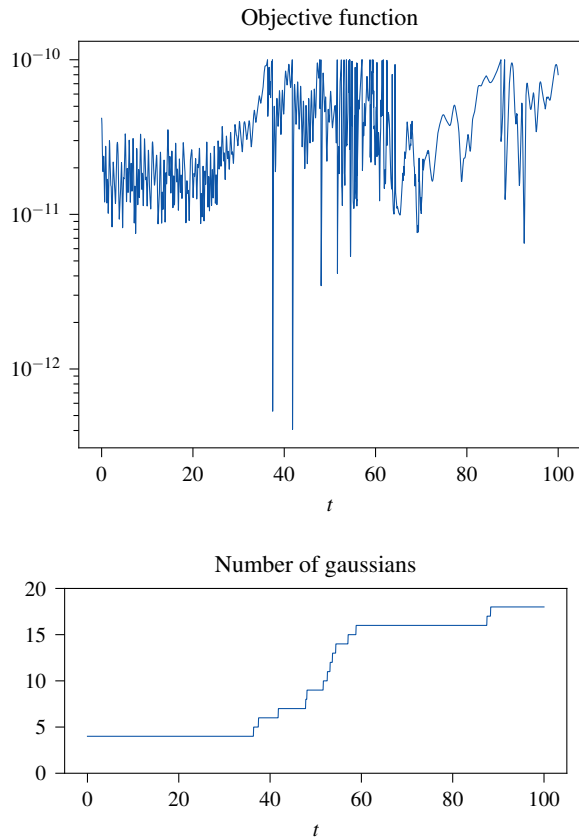


FIG. 4. Objective function and number of gaussians as a function of time during the LCG propagation using Rothe's method.

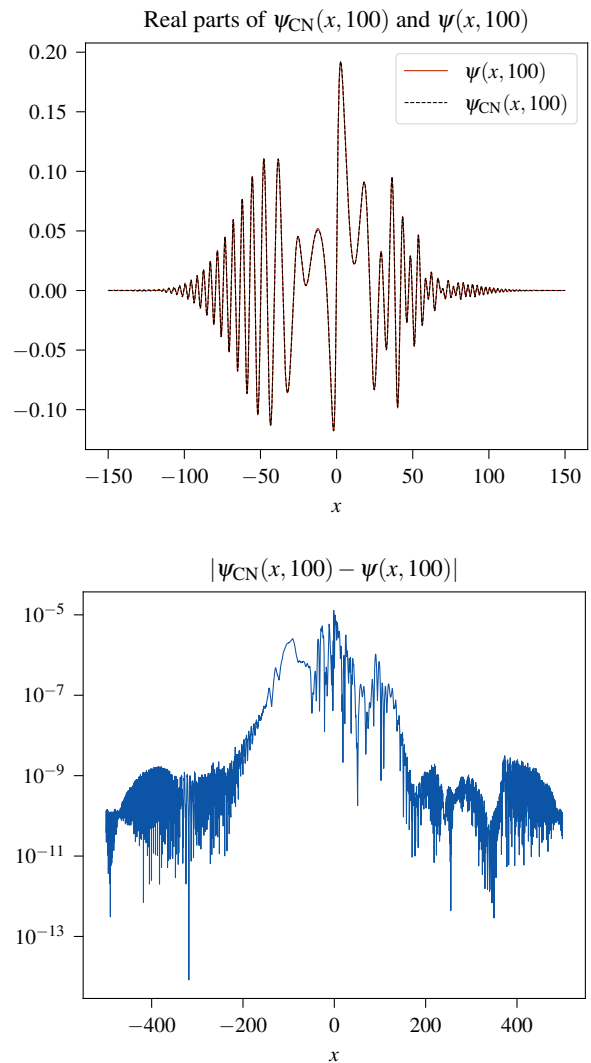


FIG. 6. Top: Real parts of final wave functions. At the resolution of the plot, no difference can be seen. Bottom: absolute value squared of the error in the final wave function.

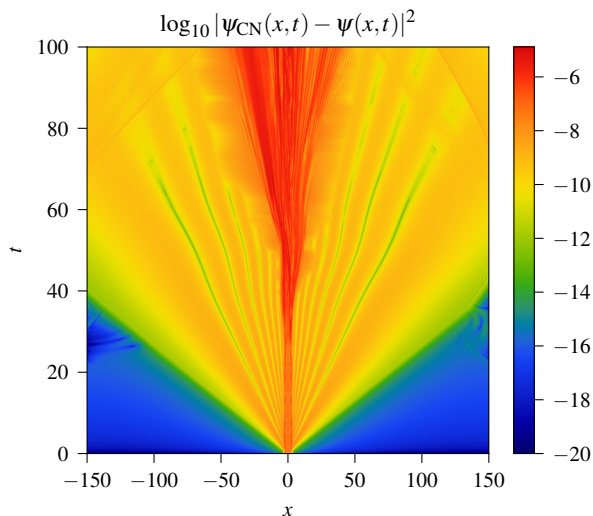


FIG. 5. Local errors of the LCG propagation relative to the Crank-Nicolson propagation. Boundary artifacts from the periodic boundary conditions can be seen, but these have extremely small values.

ing a fixed basis of B-splines [29] and/or spherical harmonics have to either grid the computational box for the B-splines or to set a maximal degree for the spherical harmonics. In both cases the basis set stays fixed and has to be chosen beforehand—see, for example, [30] for a recent simulation of the hydrogen molecule exposed to an ultrashort high-intensity laser pulse. Another example is the recent work of the present authors [31] where a fixed basis set of real, shifted explicitly-correlated gaussians was used to simulate laser alignment of the HD molecule without the Born-Oppenheimer approximation. Alternative approaches, like the time-dependent R-matrix method [32], the time-dependent surface flux method (t-SURFF) [33], or the exterior complex-scaling method [34], alleviate the inherent limitations of fixed basis sets by a sophisticated approximation of the dynamics in an a priori defined outer region. However, all state-of-the-art

methods lack real-time monitoring of the numerical time-propagation error, a hallmark of Rothe’s method as implemented here.

IV. CONCLUSION

We have demonstrated that a grid-free propagation scheme for linear combinations of complex gaussians is possible using Rothe’s method. We have introduced an efficient time-integration method that approximates the Crank–Nicolson scheme. Our initial investigation shows that this approach is robust and, with just 18 gaussians, complicated wave-function dynamics of a hydrogenic 1D model driven by an extreme laser pulse can be simulated with very high and controllable accuracy. To our knowledge, propagating an LCG wave-function *Ansatz* with this many flexible gaussians has never been successfully done within the framework of the Dirac–Frenkel principle. The scheme can be straightforwardly generalized to

realistic models of many-particle atoms and molecules using explicitly correlated gaussians within or without the Born–Oppenheimer approximation. Thus, the need for a large grid to accurately resolve local details of the time-evolving wave function, including dynamics that involve continuous parts of the spectrum such as ionization and dissociation, can be completely eliminated.

ACKNOWLEDGMENTS

The authors acknowledge the support of the Centre for Advanced Study in Oslo, Norway, which funded and hosted our CAS research project *Attosecond Quantum Dynamics Beyond the Born–Oppenheimer Approximation* during the academic year 2021/2022. The work was supported by the Research Council of Norway through its Centres of Excellence scheme, Project No. 262695. Partial support from the National Science Foundation (grant No. 1856702) is also acknowledged.

-
- [1] M. Nisoli, P. Decleva, F. Calegari, A. Palacios, and F. Martín. Attosecond Electron Dynamics in Molecules. *Chem. Rev.*, 117:10760–10825, 2017.
- [2] J. Mitroy, S. Bubin, W. Horiuchi, Y. Suzuki, L. Adamowicz, W. Cencek, K. Szalewicz, J. Komasa, D. Blume, and K. Varga. Theory and application of explicitly correlated Gaussians. *Rev. Mod. Phys.*, 85:693–749, 2013.
- [3] S. Bubin and L. Adamowicz. Matrix elements of N-particle explicitly correlated gaussian basis functions with complex exponential parameters. *J. Chem. Phys.*, 124:224317, 2006.
- [4] P. A. M. Dirac. Note on exchange phenomena in the Thomas atom. *Math. Proc. Cambridge Philos. Soc.*, 26:376–385, 1930.
- [5] J. Frenkel. *Wave Mechanics, Advanced General Theory*. Clarendon Press, Oxford, 1934.
- [6] A. D. McLachlan. A variational solution of the time-dependent Schrödinger equation. *Mol. Phys.*, 8:39–44, 1964.
- [7] P. Kramer and M. Saraceno. *Geometry of the Time-Dependent Variational Principle in Quantum Mechanics*. Springer-Verlag, Berlin, 1981.
- [8] K. G. Kay. The matrix singularity problem in the time-dependent variational method. *Chem. Phys.*, 137:165–175, 1989.
- [9] K. Rowan, L. Schatzki, T. Zaklama, Y. Suzuki, K. Watanabe, and K. Varga. Simulation of a hydrogen atom in a laser field using the time-dependent variational principle. *Phys. Rev. E*, 101:023313, 2020.
- [10] G. W. Richings, I. Polyak, K. Spinlove, G.A. Worth, I. Burghardt, and B. Lasorne. Quantum dynamics simulations using Gaussian wavepackets: the vMCG method. *Int. Rev. Phys. Chem.*, 34:269–308, 2015.
- [11] E. Rothe. Zweidimensionale parabolische Randwertaufgaben als Grenzfall eindimensionaler Randwertaufgaben. *Math. Ann.*, 102:650–670, 1930.
- [12] P. Deuffhard and M. Weiser. *Adaptive numerical solution of PDEs*. De Gruyter textbook. De Gruyter, Berlin, 2012.
- [13] S. Bubin, M. Pavanello, W.-C. Tung, K. L. Sharkey, and L. Adamowicz. Born–Oppenheimer and Non-Born–Oppenheimer, Atomic and Molecular Calculations with Explicitly Correlated Gaussians. *Chem. Rev.*, 113:36–79, 2013.
- [14] M. Bachmayr, H. Chen, and R. Schneider. Error Estimates for Hermite and Even-Tempered Gaussian Approximations in Quantum Chemistry. *Numer. Math.*, 128:137–165, 2014.
- [15] C. Lasser and C. Lubich. Computing Quantum Dynamics in the Semiclassical Regime. *Acta Numer.*, 29:229–401, 2020.
- [16] S. Bubin and L. Adamowicz. Energy and energy gradient matrix elements with N-particle explicitly correlated complex Gaussian basis functions with L=1. *J. Chem. Phys.*, 128:114107, 2008.
- [17] S.-I. Sawada, R. Heather, B. Jackson, and H. Metiu. A strategy for time dependent quantum mechanical calculations using a gaussian wave packet representation of the wave function. *J. Chem. Phys.*, 83:3009–3027, 1985.
- [18] X. Kong, A. Markmann, and V. S. Batista. Time-Sliced Thawed Gaussian Propagation Method for Simulations of Quantum Dynamics. *J. Phys. Chem. A*, 120:3260–3269, 2016.
- [19] M. A. C. Saller and S. Habershon. Quantum Dynamics with Short-Time Trajectories and Minimal Adaptive Basis Sets. *J. Chem. Theory Comput.*, 13:3085–3096, 2017.
- [20] M. H. Lee, C. W. Byun, N. N. Choi, and D. S. Kim. Solving Time-dependent Schrödinger Equation Using Gaussian Wave Packet Dynamics. *J. Korean Phys. Soc.*, 73:1269–1278, 2018.
- [21] T. Murakami and T. J. Frankcombe. Accurate quantum molecular dynamics for multidimensional systems by the basis expansion leaping multi-configuration Gaussian (BEL MCG) method. *J. Chem. Phys.*, 149:134113, 2018.
- [22] L. Joubert-Doriol. Variational Approach for Linearly Dependent Moving Bases in Quantum Dynamics: Applica-

- tion to Gaussian Functions. *J. Chem. Theory Comput.*, 18:5799–5809, 2022.
- [23] M. Dutra, S. Garashchuk, and A. V. Akimov. The quantum trajectory-guided adaptive Gaussian methodology in the Libra software package. *Int. J. Quantum Chem.*, page e27078, 2022. (In press).
- [24] I. Gutiérrez and C. Mendl. Real time evolution with neural-network quantum states. *Quantum*, 6:627, 2022.
- [25] K. Varga and J. A. Driscoll. *Computational Nanoscience: Applications for Molecules, Clusters, and Solids*. Cambridge University Press, 2011.
- [26] G. H. Golub and V. Pereyra. The Differentiation of Pseudo-Inverses and Nonlinear Least Squares Problems Whose Variables Separate. *SIAM J. Numer. Anal.*, 10:413–432, 1973.
- [27] J. Nocedal and S. J. Wright. *Numerical Optimization*. Springer Series in Operation Research and Financial Engineering. Springer, New York, NY, 2nd edition, 2006.
- [28] C. A. Floudas and P. M. Pardalos, editors. *Encyclopedia of Optimization*. Springer Reference. Springer, New York, 2nd edition, 2009.
- [29] H. Bachau, E. Cormier, P. Decleva, J. E. Hansen, and F. Martín. Applications of B-splines in atomic and molecular physics. *Rep. Prog. Phys.*, 64:1815–1943, 2001.
- [30] A. Sopena, F. Catoire, A. Palacios, F. Martín, and H. Bachau. Asymmetric electron angular distributions in H_2 induced by intense ultrashort soft-x-ray laser pulses. *Phys. Rev. A*, 105:033104, 2022.
- [31] L. Adamowicz, S. Kvaal, C. Lasser, and T. B. Pedersen. Laser-induced dynamic alignment of the HD molecule without the Born–Oppenheimer approximation. *J. Chem. Phys.*, 157:144302, 2022.
- [32] M. A. Lysaght, H. W. van der Hart, and P. G. Burke. Time-dependent R -matrix theory for ultrafast atomic processes. *Phys. Rev. A*, 79:053411, 2009.
- [33] L. Tao and A. Scrinzi. Photo-electron momentum spectra from minimal volumes: the time-dependent surface flux method. *New J. Phys.*, 14:013021, 2012.
- [34] E. Fomouo, G. L. Kamta, G. Edah, and B. Piraux. Theory of multiphoton single and double ionization of two-electron atomic systems driven by short-wavelength electric fields: An ab initio treatment. *Phys. Rev. A*, 74:063409, 2006.